



Full Length Article

A Comparative Study on Monitoring Leaf-scale Wheat Aphids using Pushbroom Imaging and Non-imaging ASD Field Spectrometers

JIN-LING ZHAO[†], DONG-YAN ZHANG^{†‡}, JU-HUA LUO[†], HAO YANG[†], LIN-SHENG HUANG[†] AND WEN-JIANG HUANG^{1†}
Institute of Remote Sensing Applications, Chinese Academy of Sciences, P.R. China

[†]*Beijing Research Center for Information Technology in Agriculture, Beijing Academy of Agriculture and Forestry Sciences, P.R. China*

[‡]*Institute of Agricultural Remote Sensing & Information Technology Application, Zhejiang University, Hangzhou, P.R. China*

¹Corresponding author's e-mail: yellowstar0618@163.com

ABSTRACT

Present paper provides information on comparing the spectral characteristics of leaf-scale wheat aphids using simultaneously the imaging Pushbroom Imaging Spectrometer (PIS) and non-imaging ASD (Analytical Spectral Devices) Fieldspec-FR2500 field spectrometer. Comparative results indicated that the PIS proved superior to the ASD in spectral resolution and sampling interval, but it was inferior in spectral range and field of view (FOV). Moreover, corresponding spectral properties were fairly similar including reflectance, spectral difference and change rate and the sensitive bands and spectral ranges. Spectral curves from both devices showed the typical reflectance properties of green vegetation: green peak at 550 nm, red valley at 680 nm and high near-infrared reflectance at 780 nm. However, the specific reflectance values appeared different for four damage levels (Normal, Light, Moderate & Serious). The maximum and minimum reflectance values were respectively 41.18% and 2.36% for the PIS, while they were 40.32% and 1.51% for the ASD, respectively. Specifically, in the wavelength range of 400-900 nm, they were similar in the spectral difference and change rate. The maximum values were respectively 14.8% and 14.0 % for the PIS, and they were 8.7% and 20.3% for the ASD, respectively. Additionally, continuum removal was used to compare the selection of sensitive bands and ranges, which were 500 nm and 663 nm, 430-530 nm and 550-690 nm for the ASD, while they were 504 nm and 681 nm, 430-530 nm and 550-730 nm for the PIS, respectively. Finally, using the high spatial resolution PIS image, environment for visualizing images (ENVI-EX) was also used to extract aphids. Overall accuracy attained was thus 97%. This study can explore further investigations in precision agriculture using near-ground imaging spectrometers. © 2012 Friends Science Publishers

Key Words: Leaf-scale wheat aphids; Analytical-spectral-device field spectrometer; Pushbroom imaging spectrometer

INTRODUCTION

Wheat (*Triticum aestivum* L.) is an important cereal crop and such as, widely cultivated throughout the world. Aphids (*Rhopalosiphum padi* L.) occurring in this crop cause significant losses in both productivity and quality. To inhibit production losses and ensure food safety, some effective measures must be taken. However, traditional field survey methods strongly depend on on-farm diagnosis of insect stress in practical farming activities. They are usually labor-intensive and time-consuming and cannot yield extensive spatial coverage (Lucas, 2011). Generally, the infestation severity of wheat aphids are observed by randomly collecting dozens of points in a field survey, therefore, it is difficult to achieve desirable conditions of aphids in a certain area, particularly for large-scale regional monitoring. Insects in wheat will spread at a fast pace and

serious hazards can be caused if they are not timely detected and prevented. Moreover, in the absence of accurate tempo-spatial distribution of wheat aphids, it usually misses the optimum chance for wheat to prevent and protect from being infested by aphids. Therefore, it is pertinent to non-destructively detect and evaluate the wheat aphids for ensuring the pesticide application remains limited and more time- and site-specifically (Delalieux *et al.*, 2009).

As compared with the more labor-intensive field work of conventional survey, quantitative remote sensing has furnished better advances in monitoring and identifying wheat aphids. For detecting crop stress using remote sensing technology, it is based on the assumption that stress factors destroy the physical structure and affect the photosynthesis of the plants. The absorption of light energy is badly influenced and thus causes spectral differences of reflectance spectra of the plants with different damage levels

(Moran *et al.*, 1997). When wheat is infested by aphids, the reflectance spectra can clearly detect differences between healthy and aphid-infested wheat. Consequently, the health status of wheat can be determined by reliably measuring the reflectance spectra. Many studies have shown that remote sensing especially the near-ground hyperspectral imaging techniques can detect pest- and disease-infested crop in a non-invasive and non-destructive way (Nillson, 1995; Mirik *et al.*, 2006; Singh *et al.*, 2010). Previous studies, using multi-spectral imaging systems, commonly collected remote sensing data for diagnosing insect stressed plants in several spectral bands in the visible and near-infrared electromagnetic regions. However, crude spectral resolution seems to be a primary limiting factor to identify subtle spectral differences for multispectral sensor systems (Govender *et al.*, 2006). Therefore, hyperspectral remote sensing, also known as imaging spectroscopy, is currently being investigated by researchers and scientists with regard to the detection and identification of plant health/stress status (Bravo *et al.*, 2003; Huang *et al.*, 2007; Yang, 2010).

Hyperspectral imaging sensor can obtain simultaneously image and spectroscopy in a single scanning process, which usually comprises about hundreds of spectral bands of relatively narrow bandwidths as well as high spatial resolution images. It can be an effective tool in describing the variability between infested and healthy wheat. Furthermore, it can provide accurate diagnosis information such as water, nitrogen, chlorophyll, pigment, etc. in the wheat growing process (Riedell & Blackmer, 1999). In the past several decades, airborne and spaceborne multi- and hyper-spectral imagery, especially non-imaging hyperspectral sensors such as the ASD field spectrometer (Analytical Spectral Devices, Inc.), have been widely used in identifying plant insects and diseases and monitoring their health status (Elliott *et al.*, 2007; Mirik *et al.*, 2007; Yang *et al.*, 2009). However, near-ground hyperspectral imaging techniques have not been fully explored in detecting wheat aphids (Inoue & Penuelas, 2001; Ye *et al.*, 2008; Zhang *et al.*, 2010). Aim of this study was to assess comparatively the spectral characteristics of leaf-scale wheat aphids using imaging and non-imaging hyperspectral data.

MATERIALS AND METHODS

Description of near-ground hyperspectral systems: The near-ground hyperspectral imaging system used in this study is the Pushbroom Imaging Spectrometer (PIS), which acquires images by linear array push-broom imaging (Fig. 1). It was jointly developed by Beijing Research Center for Information Technology in Agriculture and University of Science and Technology of China. Before using this device to scan aphid-infested wheat leaves, strict laboratory calibration were performed to accurately find out the location of each channel and ensure a high radiometric accuracy. The non-imaging spectrometer used here is the ASD Fieldspec-FR2500. Table I shows a comparative of

specification parameters between the PIS and the ASD. It is obvious that ASD has wider spectral range and larger FOV (Field of View) than that of PIS, but PIS is superior to ASD in spectral resolution and sampling interval. In addition, for a target plant, PIS can also acquire spectro-images with a very high spatial and spectral resolution by which features of interest can be identified, but ASD can only collect a mixed spectrum including target spectrum and surrounding background.

Experimental design: An experiment was conducted at the experimental farm of Beijing Academy of Agriculture and Forestry Sciences (39.93°N, 116.27°E) on 26 May 2010. At that moment, it was just the grain-filling stage of wheat. This stage is the key yield forming period, which is also extremely sensitive to various kinds of biological disasters in wheat. In this study, leaf-scale comparative study was performed concerning aphid-infested wheat using the PIS and the ASD spectrometers simultaneously. When aphid-induced symptoms of wheat leaves were assessed, relative pest damage levels were estimated according to the aphid populations. To keep the leaves fresh, PIS was set up in a dark room near the experimental farm. Subsequently, the inverse 2nd leaves were picked up and immediately put onto the scanning platform. After collecting the reflectance spectra, the PIS lens was set at 80 cm over the aphid-infested wheat leaves and halogen lamp irradiation was fixed at a 45° angle. To reduce random errors, seven groups of leaves were measured with different aphid damage levels. Before and after collecting the leaf spectra, white reference panel was used to optimize the instrument.

Data acquisition and preprocessing: When data collection was performed, PIS moved evenly along the track and the spectra of wheat leaves were acquired on the black cloth (Fig. 1). After leaves were scanned using PIS, ASD was immediately used to collect the spectra by measuring each leaf ten times from the leaf tip to the bottom, and the average was used as the final reflectance. Original spectra were measured, further processing must be required to convert the original radiance values to reflectance. The reflectance conversion from PIS was performed by the empirical linear method (Eq. 1). Then, a moving-average smoothing algorithm for the PIS images was utilized to exclude abnormal values and smooth spectral curves in order to derive the reflectance characteristics between healthy and aphid-infested wheat leaves. Furthermore, data analysis and spectral curves drawing were performed with Origin 8 (OriginLab).

$$\rho = a * DN + b \quad (1)$$

Where ρ is the real reflectance, a and b are the coefficients. When putting the measured spectral value and corresponding DN (digital number) into Eq. 1, a and b can be obtained by Least-square Method (LSM) and then ρ can be gotten.

Likewise, for the ASD reflectance conversion, ASD-viewspec Pro 6.0.11 program was used to export original

spectral data to Microsoft Excel software and Eq. 2 was used to derive the converted reflectance.

$$R_t = \frac{\text{Rad}_t}{\text{Rad}_r} \times R_r \times 100\% \quad (2)$$

Where R_t is the target's calibrated reflectance using the white reference panel, Rad_t is the target's radiance values acquired by ASD, Rad_r is the radiance values of the white reference panel and R_r is the known reflectance of the white reference panel.

Concerning the spectral response induced by wheat aphids, the selection and difference of sensitive bands and spectral range were compared using two devices. In our study, continuum removal was used to identify spectral bands and ranges sensitive to different aphid damage levels. This method is actually an extrapolation of the baseline of a specific curve, which extends across the base of absorption bands by fitting the smoothed curve to the general trend. The first and last spectral data are on the hull, so the first and last bands in the output continuum-removed data file are converted to 1.0. Furthermore, the calculation equation of depth (D) for an absorption band is shown in Eq. 3. Kokaly and Clark (1999) were the first researchers to use the method in vegetation studies when estimating nitrogen, lignin and cellulose concentrations in dried ground leaves.

$$D = 1 - R_b / R_c \quad (3)$$

Where R_b is the reflectance at the bottom (trough center point) of the band and R_c is the continuum base.

RESULTS AND DISCUSSION

Comparative analysis of spectral characteristics: For improving mutual comparison between the PIS and the ASD, seven groups of healthy and aphid-infested wheat leaves were utilized and different aphid damage levels were merged to four severity levels and their average spectra were obtained. The spectral curves were generated using the data analysis and graphing software (Origin 8). As shown in Fig. 2, for a certain damage level, it was clear that the spectral characteristics derived from the PIS and the ASD were consistent. At 550 nm, 680 nm and 780 nm, spectral curves from both spectrometers showed the typical spectral characteristics of vegetation: green peak, red valley and high near-infrared reflectance, but specific spectral values appeared different for the same damage level. Specifically, the differences were: (1) the values derived from the PIS were bigger than that from the ASD for each damage level; (2) the maximum and minimum reflectance values were 41.18% and 2.36% for the PIS, while they were 40.32% and 1.51% for the ASD; (3) the spectral curves from the PIS were less smooth than that from the ASD due to the smoothing algorithm selection and the existence of systematic noises for the

PIS.

Additionally, the comparative analysis of spectral difference and change rate were also carried out between normal and serious levels using both spectrometers (Fig. 3). Due to larger spectral range, ASD could obtain the spectral difference in the visible, near-infrared and shortwave infrared bands, while PIS could only obtain that in the visible and partial near-infrared bands. Comparing the change characteristics in the 400-900 nm spectral regions, it could be found that they were similar in the spectral difference and change rate curves, but there were also some minor differences in the changes in extent and amplitude. For the PIS spectrometer, the maximum change rate and difference were 14.8% and 14.0%, while they were 8.7% and 20.3% for ASD.

Furthermore, the selection of spectral sensitive bands and ranges were compared between two devices. Fig. 4 is the identification results using the continuum removal method. As shown in this figure, there were two spectral sensitive ranges for both the ASD and the PIS. They were 430-530 nm and 550-690 nm, and 430-530 nm and 550-730 nm, respectively. Similarly, there were also two sensitive bands: 500 nm and 663 nm, and 504 nm and 681 nm, respectively. According to the comparative results, it could be found that both devices had very similar spectral sensitive bands and ranges in the visible spectrum. However, they were different in the near-infrared spectrum: PIS had a wider spectral sensitive range than that of ASD and its sensitive bands moved towards the red edge more far than that of ASD.

Identification of aphids using the PIS image: On the PIS image, two pixels including a normal leaf point and an aphid-covered leaf point were selected. Fig. 5 is the comparative result of spectral reflectance curves between normal and aphid-infested pixels in the 500-900 nm spectral range. As seen in Fig. 5(a), due to the influence of environmental and systematic noises, the spectral curves were badly affected by some abnormal values and they fluctuated severely, especially in the near-infrared spectrum. In order to reflect the real waveform characteristics, adjacent-averaging smoothing method was used and Fig. 5(b) was the smoothed result. It is obvious that the spectral reflectance values were markedly different between normal and aphid leaves. Between 500 and 701 nm, the reflectance of aphid leaf was larger than that of normal leaf, while it was smaller in the 701-900 nm wavelengths. In the visible spectrum (500-701 nm), the maximum delta (the maximum value minus the minimum value) was 3.33 and it was 7.47 in the near-infrared spectrum (701-900 nm). For the locations of the minimum value, they were very similar between normal and aphid points, which were 664 nm and 661 nm, respectively. However, they were very different for the locations of maximum values, which were 785 nm and 852 nm, respectively.

Table 1: A comparative of some specification parameters between imaging and non-imaging spectrometers

Sensor parameters	PIS	ASD
Spectrum range	400~1000 nm	350~2500 nm
Spectral resolution	2 nm	3 nm @ 700 nm; 10 nm @1400 nm & 2100 nm
Sampling interval	0.7 nm	1.4 nm (350-1000 nm); 2 nm (1000-2500 nm)
FOV	16°	25°
Spatial resolution	5-10 mm	-
Pixel dimension	7.4 μm×7.4 μm	-
Image resolution	1400 (Spatial dimension) × 1024 (Spectral dimension)	-

Fig. 1: A demonstration of acquiring the spectra combing with image with different aphid damage levels using PIS

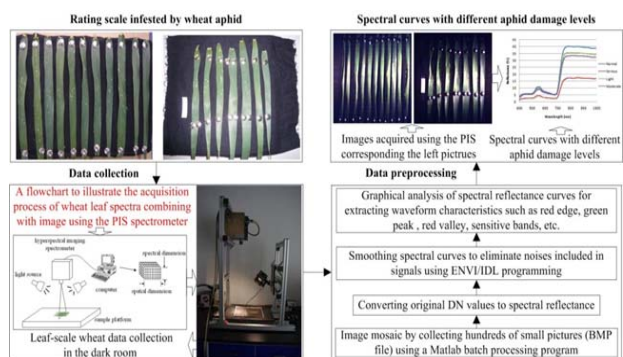
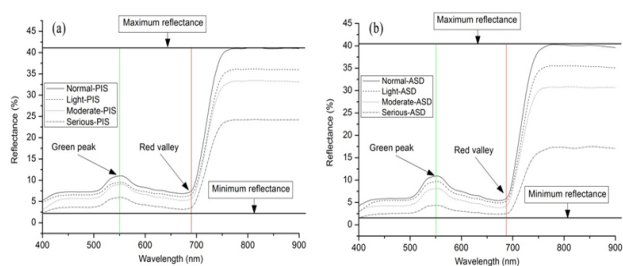


Fig. 2: A comparative of collected spectral curves with different aphid infestation using the PIS (a) and the ASD (b)



The phenomenon for the change trend was that aphids cover the top of wheat leaf and they broke the cell structure and changed chlorophyll content. Additionally, the secretions of aphids adhered to the leaf top, which could absorb some dust and other materials and resulted in the increase of reflectance. In the visible spectrum, the reflectance was mainly determined by various pigments, among which, chlorophyll was a leading one. When aphids broke the wheat leaf, chlorophyll content would accordingly decrease, which caused an increase of reflectance due to the decreasing ability of chlorophyll absorption. Conversely, the reflectance depended on the cell structure in the near-infrared spectrum. Aphids broke the cell structure of wheat leaf, so the reflectance of aphid-infested leaf

Fig. 3: A comparative analysis of spectral difference and change rate between normal and serious levels using the PIS (a) and the ASD (b)

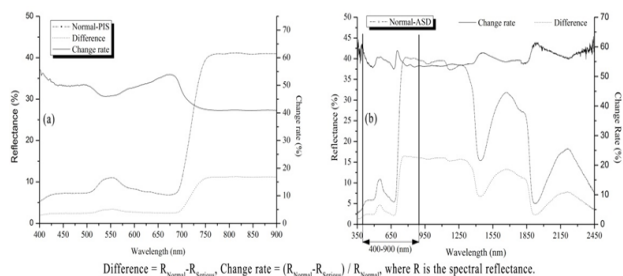
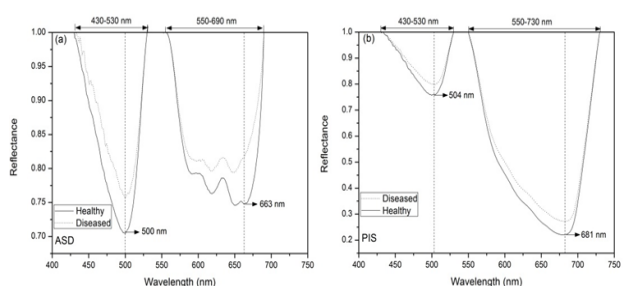


Fig. 4: A comparative of sensitive bands and spectral sensitive ranges using the ASD (a) and the PIA (b) based on the continuum removal method



decreased correspondingly compared with normal leaf.

As compared with ASD, PIS can acquire image and spectral information simultaneously, so it can be utilized to identify aphids using its high spatial resolution image. Due only to the leaf-scale analysis in this study, it was easy to separate aphids from leaf background. ENVI-EX (ENvironment for Visualizing Images, Research Systems, Inc.) feature extraction module was used due to obvious aphid texture and single background. As shown in Fig. 6(a), there were five necessary steps to complete the object-oriented classification including choosing the scale parameter, merging the object primitives, refining the objects using a threshold value for just one band of the image and it was an optional step, extraction of the attributes, and object-oriented classification based on rules or examples. As can be seen from Fig. 6(b), it was obvious that most aphids were extracted from normal wheat leaves. In order to validate the identification accuracy, 30 aphid points were randomly selected in the ENVI environment and they were then found on the classification map using link displays tool. The comparative result showed that 29 points were correctly identified and the overall accuracy reached 97%.

CONCLUSION

1. PIS is a near-ground hyperspectral imaging system, which can combine image with spectrum compared with non-imaging ASD spectrometer. In the same spectral range (400-900 nm), both the PIS and ASD have similar change

Fig. 5: The curves' comparative between normal and aphid-infested leaf on the PIS image: (a) is the pre-smooth curves and (b) is the post-smooth curves

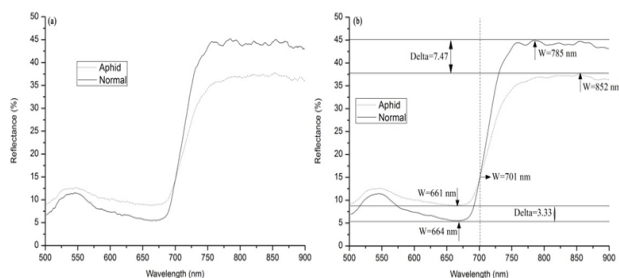
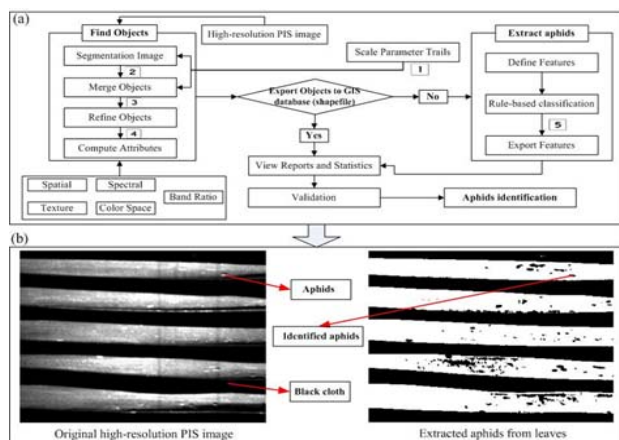


Fig. 6: Technical flowchart for identifying leaf-scale wheat aphids using the ENVI-EX object-oriented classification module (a) and the high-resolution image acquired by PIS and the identification result (b)



trends of spectral curves with different aphid damage levels, but their changes in extent and amplitude are different. Furthermore, PIS has smaller sampling interval than the ASD, so the spectral differences between normal and aphid-infested wheat leaves can be accurately detected by this device.

2. In addition, PIS can also collect the pixel-to-pixel spectra, while ASD only acquire the average spectra of a leaf. Conversely, the measured spectra using ASD are usually mixed spectral information including soil, stem, etc. When they were used to identify aphids on wheat leaves, it will inevitably exert a negative impact on the retrieval model.

3. Due to narrower spectral range than the ASD, PIS can only derive corresponding information of targets in the visible and near-infrared bands, which is also a major constraint to wide applications in precision agriculture, especially those crops that are sensitive to shortwave infrared bands. In addition, narrow swath and dozens of spectral bands are two limiting factors to create large dataset, which requires finding out effective and fast algorithms for data compression and band selection in the future researches.

Acknowledgement: The project was supported by China Postdoctoral Science Foundation funded project (20110490317), National Natural Science Foundation of China (41071276, 41101395), Program of Ministry of Agriculture (200903010), Special Funds for Major State Basic Research Project (2007CB714406), and Postdoctoral Science Foundation of Beijing Academy of Agriculture and Forestry Sciences (2011).

REFERENCES

Bravo, C., D. Moshou, J. West, A. McCartney and H. Ramon, 2003. Early disease detection in wheat fields using spectral reflectance. *Biosystems. Eng.*, 84: 137–145

Delalieux, S., A. Auwerkerken, W.W. Verstraeten, B. Somers, R. Valcke, S. Lhermitte, J. Keulemans and P. Coppin, 2009. Hyperspectral reflectance and fluorescence imaging to detect scab induced stress in apple leaves. *Remote Sens.*, 1: 858–874

Elliott, N., M. Mirik, Z. Yang, T. Dvorak, M. Rao, J. Michels, T. Walker, V. Catana, M. Phoofole and K. Giles, 2007. Airborne multi-spectral remote sensing of Russian wheat aphid injury to wheat. *Southwest. Entomol.*, 32: 213–219

Govender, M., K. Chetty and K. Bulcock, 2006. A review of hyperspectral remote sensing and its application in vegetation and water resource studies. *Water SA*, 33: 145–152

Huang, W.J., D.W. Lamb, Z. Niu, Y.J. Zhang, L.Y. Liu and J.H. Wang, 2007. Identification of yellow rust in wheat using in-situ spectral reflectance measurements and airborne hyperspectral imaging. *Precis. Agric.*, 8: 187–197

Inoue, Y. and J. Penuelas, 2001. An AOTF-based hyperspectral imaging system for field use in ecophysiological and agricultural applications. *Int. J. Remote Sens.*, 22: 3883–3888

Kokaly, R.F. and R.N. Clark, 1999. Spectroscopic determination of leaf biochemistry using band-depth analysis of absorption features and stepwise multiple linear regression. *Remote Sens. Environ.*, 67: 267–287

Lucas, J.A., 2010. Advances in plant disease and pest management. *J. Agric. Sci.*, 149: 91–114

Mirik, M., Jr. G.J. Michels, S. Kassymzhanova-Mirik and N.C. Elliott, 2007. Reflectance characteristics of Russian wheat aphid (Hemiptera: Aphididae) stress and abundance in winter wheat. *Comput. Electron. Agric.*, 57: 123–134

Mirik, M., Jr. G.J. Michels, S. Kassymzhanova-Mirik, N.C. Elliott, V. Catana, D.B. Jones and R. Bowling, 2006. Using digital image analysis and spectral reflectance data to quantify damage by greenbug (Hemiptera: Aphididae) in winter wheat. *Comput. Electron. Agric.*, 51: 86–98

Moran, M.S., Y. Inoue and E. Barnes, 1997. Opportunities and limitations for image-based remote sensing in precision crop management. *Remote Sens. Environ.*, 61: 319–346

Nillson, H.E., 1995. Remote sensing and image analysis in plant pathology. *Annu. Rev. Phytopathol.*, 15: 489–527

Riedell, W.E. and T.M. Blackmer, 1999. Leaf reflectance spectra of cereal aphid-damaged wheat. *Crop Sci.*, 39: 1835–1840

Singh, C.B., D.S. Jayas, J. Paliwal and N.D.G. White, 2010. Identification of insect-damaged wheat kernels using short-wave near-infrared hyperspectral and digital colour imaging. *Comput. Electron. Agric.*, 73: 118–125

Yang, C.M., 2010. Assessment of the severity of bacterial leaf blight in rice using canopy hyperspectral reflectance. *Precis. Agric.*, 11: 61–81

Yang, Z., M.N. Rao, N.C. Elliott, S.D. Kindler and T.W. Popham, 2009. Differentiating stress induced by greenbugs and Russian wheat aphids in wheat using remote sensing. *Comput. Electron. Agric.*, 67: 64–70

Ye, X.J., K. Sakai, H. Okamoto and L.O. Garciano, 2008. A ground-based hyperspectral imaging system for characterizing vegetation spectral features. *Comput. Electron. Agric.*, 63: 13–21

Zhang, D.Y., X.Y. Song, Z.H. Ma, G.J. Yang, W.J. Huang and J.H. Wang, 2010. Assessment of the developed pushbroom imaging spectrometer in single leaf scale (In Chinese). *Sci. Agric. Sin.*, 43: 2239–2245

(Received 10 September 2011; Accepted 28 November 2011)